Incipient ferroelectric to a possible ferroelectric transition in Te^{4+} doped calcium copper titanate ($CaCu_3Ti_4O_{12}$) ceramics at low temperature as evidenced by Raman and dielectric spectroscopy

Nabadyuti Barman, Priyank Singh, Chandrabhas Narayana, and K. B. R. Varma

Citation: AIP Advances **7**, 035105 (2017); doi: 10.1063/1.4973645
View online: https://doi.org/10.1063/1.4973645
View Table of Contents: http://aip.scitation.org/toc/adv/7/3
Published by the American Institute of Physics

Incipient ferroelectric to a possible ferroelectric transition in Te^{4+} doped calcium copper titanate ($CaCu_3Ti_4O_{12}$) ceramics at low temperature as evidenced by Raman and dielectric spectroscopy

Nabadyuti Barman,[1] Priyank Singh,[2] Chandrabhas Narayana,[2,a] and K. B. R. Varma[1,b]
[1]*Materials Research Center, Indian Institute of Science, Bangalore 560012, India*
[2]*Light Scattering Laboratory, Chemistry and Physics of Materials Unit, Jawaharlal Nehru Centre for Advanced Scientific Research (JNCASR), Bangalore 560064, India*

(Received 10 October 2016; accepted 22 December 2016; published online 6 March 2017)

Partial replacement of Ti^{4+} by Te^{4+} ions in calcium copper titanate lattice improved its dielectric behaviour mostly due to cubic-to-tetragonal structural transformation and associated distortion in TiO_6 octahedra. The relative permittivity values (23–30 x 10^3) of Te^{4+} doped ceramics is more than thrice that of un-doped ceramics (8 x 10^3) at 1 kHz. A decreasing trend in relative permittivity with increasing temperature (50–300 K) is observed for all the samples. Barrett's formula, as a signature of incipient ferroelectricity, is invoked to rationalize the relative permittivity variation as a function of temperature. A systematic investigation supported by temperature dependent Raman studies reveal a possible ferroelectric transition in Te^{4+} doped ceramic samples below 120 K. The possible ferroelectric transition is attributed to the interactions between quasi-local vibrations associated with the micro-clusters comprising TiO_6 and TeO_6 structural units and indirect dipole-dipole interactions of off-center B–cations (Ti^{4+} and Te^{4+}) in double perovskite lattice. [http://dx.doi.org/10.1063/1.4973645]

I. INTRODUCTION

Thin-films and hetero-structures based on perovskite oxide ferroelectrics have been the subject of extensive study as these are of potential importance for a wide variety of device applications that include non-volatile ferroelectric memories, dynamic random access memories, tunable microwave devices *etc*.[1–3] Recently, there is an increasing interest on $CaTiO_3$ or $SrTiO_3$ type materials, which are known to be incipient ferroelectrics,[4,5] owing to their tremendous potential for device applications. Generally, centrosymmetric ABO_3 type perovskites containing d^0 cations at B-site, i.e., Ti^{4+}, Ta^{5+}, Nb^{5+} *etc*., with polarizable BO_6 octahedra are classic examples of incipient ferroelectrics.[6–8] The intrinsic tilt associated with BO_6 octahedra plays an important role in exhibiting the incipient behaviour. Incipient ferroelectric materials exhibit a rise in permittivity (ε′) value on cooling towards 0 K owing to quantum fluctuations.[9] According to the reports in the literature, insertion of small amounts of dopants at A or B-site of these incipient ferroelectrics has a profound effect on their dielectric and structural properties, *viz*, triggers relaxor or ferroelectric behaviour.[10,11]

In cubic double perovskite $AA'_3B_4O_{12}$ family, a dubious compound calcium copper titanate ($CaCu_3Ti_4O_{12}$, CCTO) drew the attention of many researchers around the globe.[12] There exists ample literature on structural and physical properties (especially dielectric) of this compound with no

[a]Email: cbhas@jncasr.ac.in
[b]Email: kbrvarma@mrc.iisc.ernet.in

undisputed conclusions. Among all the physical properties reported, the high permittivity associated with this compound has been very intriguing as this material was known to belong to nonpolar crystal class. Though our group reported various physical properties of this material, the specific report concerning the incipient ferroelectric characteristics of CCTO prompted us to take up the investigations that are reported over here.[10–12] It was demonstrated that the permittivity (ε_r) value associated with the bulk response (10-120 K) decreases with increasing temperature for both single crystals (10–55 K) and ceramics (60–110 K) of CCTO which is consistent with incipient ferroelectricity obeying the Curie-Weiss law with a negative Curie temperature. This result facilitated establishing the structure-property correlations similar to that of many other titanate-based perovskites associated with B-site octahedral tilting. The temperature dependence of ε_r and the Curie-Weiss behaviour of a particular doping concentration of Mn^{2+} at A′-site (Cu-site) indicate the possible existence of incipient ferroelectricity in Mn-doped CCTO ceramics although the origin of incipient ferroelectricity was barely enlightened.[13]

There was a recent report on $ACu_3Ti_4O_{12}$ family with Na^+ and Bi^{3+} occupying A site, *i.e.*, $Na_{0.5}Bi_{0.5}Cu_3Ti_4O_{12}$ (NBCTO) which is iso-structural with CCTO with $Im\bar{3}$ cubic symmetry and is known to be an incipient ferroelectric.[14] The infrared and terahertz spectroscopic data of NBCTO revealed the splitting and softening of low frequency modes (34, 71, 100, 124 and 136 cm^{-1}) corresponding to the mixed occupancy of Na^+ and Bi^{3+} ions on the *A* site. This made us more inquisitive especially to visualize the effect of partially replacing B-site (Ti^{4+}) by Te^{4+} ($5s^2$ lone pair) in $ACu_3Ti_4O_{12}$ class of double perovskites on their structures and physical properties. The partial Te^{4+} doping at the B-site in CCTO resulted in centrosymmetric tetragonal (*I*4/*mmm*) symmetry with an increase in its dielectric tunability.[15] We present here the results pertaining to the temperature dependent dielectric and Raman spectroscopic studies carried out on undoped and doped CCTO ceramics that revealed the presence of modes associated with tetragonal (*I*4/*mmm*) crystal structure and give ample evidence for the presence of incipient ferroelectricity besides the structural transformation occurring in this compound at a low temperature.

II. EXPERIMENTAL SECTION

Polycrystalline samples of $CaCu_3Ti_{4-x}Te_xO_{12}$ (x = 0, 0.1, 0.2) were synthesized *via* solid-state reaction route using $CaCO_3$ (99.37 % Aldrich), CuO (98.7% Alfa-aser), TiO_2 (99.27 % Aldrich) and TeO_2 (99.37 % Aldrich). For this, stoichiometric amounts of these raw materials were mixed using an agate pestle and mortar. For homogenization, the mixture was ball-milled for 3–4 h. The powder thus ground was initially heated at 600 °C/6 h. Subsequently, it was cooled down to room temperature at a rate of 2 °C/min and again ball-milled for 3–4 h to further homogenize the mixture. Thus obtained powder was subjected to calcination at 980 °C/8 h and cooled down to room temperature. X-ray powder diffraction studies were carried out to confirm the desired phase formation.[15] The powder samples were cold-pressed (at room temperature) to obtain pellets of 8 mm in diameter and were sintered at 1050 °C/10 h. The density of sintered pellets was around 95–98 % as determined by the Archimedes' method.

The capacitance and dielectric loss (D) were monitored as a function of frequency (100 Hz–110 MHz) at a signal strength of 0.2 V using Agilent 4294A impedance analyzer. Low-temperature dielectric measurements were done with the aid of a cryostat of APD Cryogenics at a vacuum level of 10^{-6} Torr. For the Raman measurements, a custom built micro-Raman setup was employed; the details of which were elucidated elsewhere.[16] The samples were mounted in a liquid nitrogen-flow cryostat (Linkam make) and the spectra were recorded in backscattering geometry using 532 nm laser as excitation. The laser beam was focused through a 50x microscope objective (Nikon make with 0.45 NA) on the sample surface. Laser power at the sample was ~ 5 mW. The scattered light was analyzed by a monochromator equipped with three-grating spectrometer and liquid nitrogen cooled charge-coupled device detector. Grating used for all the measurements was 1800 grooves/mm. Raman spectra were calibrated using Neon lamp. Raman spectra were fitted using Lorentzian profiles for determining the peak position and full width at half maximum (FWHM).

III. RESULTS AND DISCUSSION

As reported in our earlier communication,[15] $CaCu_3Ti_{4-x}Te_xO_{12}$ (x = 0.1, 0.2; CCTTO1, CCTTO2) is confirmed to crystallize in the double perovskite structure associated with the space group $I4/mmm$ (lattice parameters, a = 6.947 Å and c = 7.3939 Å) and contains two formula units per unit cell. But the pure $CaCu_3Ti_4O_{12}$ (CCTO) has cubic double perovskite structure with the space group of $Im\bar{3}$ (lattice parameter a = 7.391 Å). This structural change is suspected to influence the electrical behaviour of doped CCTO ceramics. In Figure 1(a and b), the plots of the real part of relative permittivity (ε_r) and loss (D) *versus* frequency (f) are shown at 300 K for undoped (x = 0) and Te-doped (x = 0.1, 0.2) CCTO ceramics. The Te-doped samples (CCTTO) have relative permittivity (ε_r) values in the range of ~ 20–30 x 10^3 which are much higher than that of undoped CCTO (~8 x 10^3) at 1 kHz. The relative permittivity (ε_r) *vs* frequency plots (Figure 1a) show two distinguishable relaxations (around 10^2–10^4 Hz and $5x10^5$–10^7 Hz) followed by two almost unchanging dielectric constant value region (around 10^4–$5x10^5$ Hz and 10^6–10^8 Hz) for undoped and doped samples. The mid-frequency regime, *i.e.*, 10^4 to $5x10^5$ Hz, dielectric constant values of around 16000 for CCTTO2, 12000 for CCTTO1 and 7000 for CCTO are attributed to the permittivity response of insulating grain boundaries (GB) in the ceramic samples. In the frequency range (>$5x10^5$ Hz), Maxwell-Wagner type relaxation is evidenced in all the ceramics. The high frequency dielectric constant (for instance, >$5x10^6$ Hz for CCTTO1 and CCTTO2, >$3x10^6$ for CCTO) corresponding to the semiconducting grain (bulk) is encountered owing to the step-like behavior of relative permittivity of undoped and doped CCTO samples.[17] However, the intrinsic grain permittivity values for pure and doped samples are relatively small when compared to the giant extrinsic values (at lower frequencies). For example, the intrinsic bulk permittivity (ε_r) at 10 MHz is ~ 120 for $CaCu_3Ti_4O_{12}$ (CCTO), ~ 190 for $CaCu_3Ti_{3.9}Te_{0.1}O_{12}$ (CCTTO1) and ~ 450 for $CaCu_3Ti_{3.8}Te_{0.2}O_{12}$ (CCTTO2). Nevertheless, the bulk and the GB permittivity for the CCTTO samples are higher than that of the pure one.

Figure 2a shows the variation of relative permittivity (ε_r) associated with the bulk response (at 1 MHz) for two different Te doped samples within the temperature range of 50–300 K. For CCTTO1 and CCTTO2 samples, the relative permittivity increases sluggishly on increasing the temperature upto 150 K and undergoes a broad maximum (T_m) in the 75 to 175 K temperature range. On increasing the dopant concentration, the T_m shifts to higher temperature; for instance, the T_m for CCTTO1 is centred around 130 K while it is 170 K for CCTTO2. The pure sample (CCTO) shows almost invariant ε_r behaviour (with a little decrease in permittivity value) with increasing temperature. Dielectric behaviour of doped samples confirms polarization increase with a decrease in temperature (limited range) which is very similar to the anomalous dielectric behaviour of incipient ferroelectric or ferroelectric perovskite oxides in the low temperature region (0–250 K).

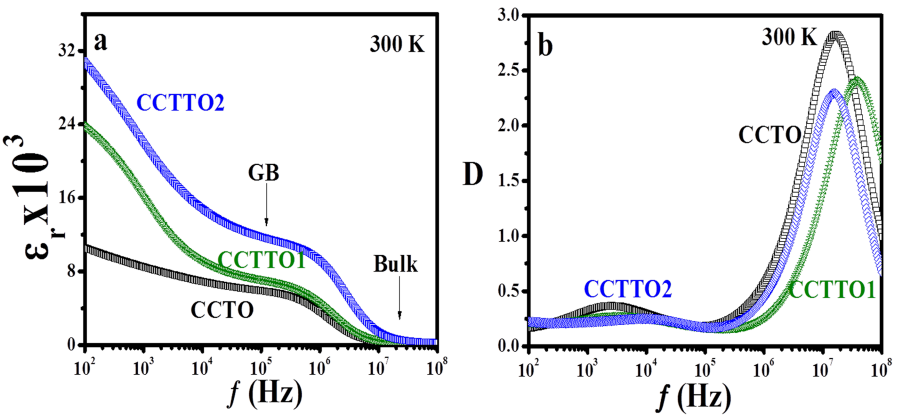

FIG. 1. (a) Relative permittivity (ε_r) and loss (D) (b) as a function of frequency for the $CaCu_3Ti_{4-x}Te_xO_{12}$ ceramics sintered at 1050 °C for x = 0 (CCTO), 0.1 (CCTTO1) and 0.2 (CCTTO2), measured at 300 K.

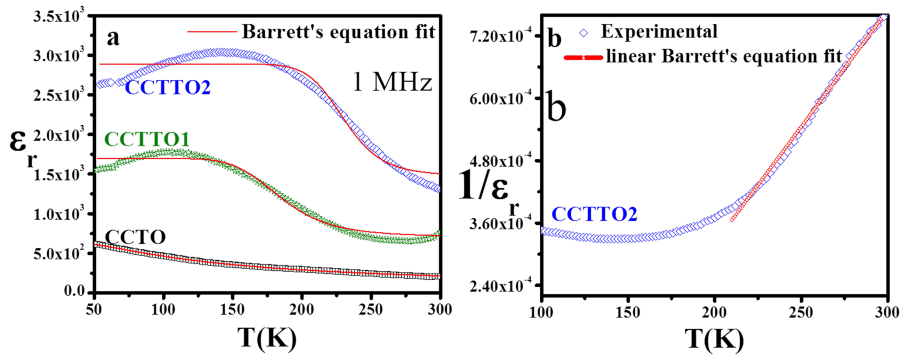

FIG. 2. a) Temperature dependent real part of permittivity (ε_r) for $CaCu_3Ti_{4-x}Te_xO_{12}$ (x = 0, 0.1, 0.2) with its Barrett's equation fit at fixed frequency of 1 MHz b) linear Barrett fit for CCTTO2.

The dielectric behaviour of the incipient ferroelectrics at low-temperatures can be fitted according to the Barrett's equation as given below;[18,19]

$$\varepsilon = A + \frac{C}{\frac{T_1}{2} coth\left(\frac{T_1}{2T}\right) - T_0} \tag{1}$$

where, T_1 is quantum fluctuations temperature (QFT), T_0 is the ferroelectric transition temperature (FTT), C is the Curie constant, A is temperature independent part of dielectric constant. In the high temperature (T) limit, the classical result is restored as $\varepsilon \approx C/T_1 - T_0$ and in the low T limit, the equation saturates with $\varepsilon \approx 2C/T_1 - 2T_0$. So, it may be concluded from Barrett's equation that T_1 is the dividing point between classical and non-classical behaviour. In the high temperature ($T>T_1$) limit, the classical result is restored as $\varepsilon \approx C/T_1 - T_0$ and the Curie-Weiss law is valid. Therefore, in a material undergoing a transition to the ferroelectric state at a finite temperature above T_1, the quantum effect will be unobserved.

In the low temperature region the equation saturates with $\varepsilon \approx 2C/T_1 - 2T_0$. For $T<T_1$, in the low temperature region, the quantum effect is important and permittivity (polarization) deviates from Curie-Weiss law. In many cases, T_0 is ≤ 0 K, which refers to non-real transition temperature. Therefore, the material does not undergo a ferroelectric phase transition at any finite temperature. When, T_0 is finite and $T_0 < T_1$, the quantum fluctuations that occur below T_1 break the long-range ferroelectric order and stabilize the quantum paraelectric state in the sample and a probable ferroelectric transition occurs at T_0.[14,18]

The dielectric data for CCTO, CCTTO1 and CCTTO2 are fitted using Equation. (1) as shown in Figure. 2a, which shows a good fit for the dielectric data obtained for CCTO sample over the temperature range of 50–300K, but the dielectric data for CCTTO1 and CCTTO2 deviate from the fit throughout the temperature range covered in the present study. The linear Barret formula fits well in the temperature range of 250–170 K for CCTTO2 (Figure. 2b) and 250–140 K for CCTTO1 samples (Figure. S1 of the supplementary material). The fitted parameters are listed in Table I.

The values, *i.e.*, $T_1 \sim -0.074$ K and $T_0 \sim -47$ K obtained for pure CCTO demonstrate that the material does not undergo a ferroelectric phase transition at any finite temperature. But, for the doped systems, like CCTTO2, both FTT and QFT are finite; *i.e.* $T_0 \sim 135$ K and $T_1 \sim 167$ K. The Te doped samples are non-ferroelectric at room temperature. Since $T_0 < T_1$ and also both T_0 and T_1 are finite for

TABLE I. Parameters of Barret fitting for $CaCu_3Ti_{4-x}Te_xO_{12}$, x = 0 (CCTO), x = 0.1 (CCTTO1) and x = 0.2 (CCTTO2).

	C (x10^4 K)	A	T_0 (K)	T_1 (K)
CCTO	5.9 ± 0.02	112	-0.074 ± 0.04	-47 ± 0.53
CCTTO1	18.5 ± 0.75	546	110 ± 2	125 ± 2
CCTTO2	22.5 ± 0.26	827	135 ± 3	167 ± 4

CCTTO1 and CCTTO2. Therefore, it is concluded that the existing long-range ferroelectric order in these Te doped samples is broken due to quantum fluctuations below 167 K. In pure CCTO, the TiO_6 octahedra show unusual tilting of 23° ($a^+ a^+ a^+$) in $Im\bar{3}$ cubic symmetry.[19] The Glazer tilt angle of BO_6 octahedra in tetragonal *I*4/*mmm* symmetry is calculated to be 24.6° ($a^0 b^+ b^+$) for CCTTO samples.[15] As the octahedral tilt angle is larger for Te doped samples as compared to that of pure CCTO, one could expect high displacive polarizability from "rattling" cation (Ti^{4+} and Te^{4+}) in octahedral cage arising from locally stretched lattice for Te-doped samples. As a result, the dielectric response in the grains (at 1 MHz) is ~ 4 to 5 times higher in CCTTO2 than that of CCTO (Figure 2a). However, larger cationic radius and different electronic structure of Te^{4+} (0.91 Å) compared to Ti^{4+} (0.61 Å) results in different hybridization with the O^{2-} ions. The octahedral distortions of TiO_6 and TeO_6 along with different hybridizations result in the formation of different polar micro-clusters. Even, electron lone pair associated with Te^{4+} ions coupled with the mass difference helps in the enhancement of polarizability of BO_6 octahedra. Polar micro-clusters, resulting from different chemical bonding and steric effect of lone pair, also have pronounced effect on room temperature relative permittivity value. Also, the polar ordering upon cooling of these above mentioned micro-clusters gives rise to an increase in relative permittivity. Finite T_0 and T_1 values and large increase in bulk/grain permittivity value for both CCTTO1 and CCTTO2 as compared to that of undoped CCTO supports the fact that the distorted BO_6 octahedra (due to Te doping) are the origin of intrinsic polar regions in tetragonal I4/mmm double perovskite.

It is interesting to note that the relative permittivity value tends to decrease for both CCTTO1 and CCTTO2 samples below 120 K deviating from Barrett's fit. It suggests that along with polar ordering, possible ferroelectric phase transition (at T_0) might be occurring around 120 K. It is conjectured based on the broadness associated with the permittivity peak that the transition may be second-order in nature. To have further insights into this phenomenon, temperature dependent Raman spectroscopic analyses were taken up and the details of which are elucidated in the following section.

Raman spectra for CCTO, CCTTO1 and CCTTO2 in the $CaCu_3Ti_{4-x}Te_xO_{12}$ polycrystalline samples were obtained at room temperature (see Figure 3 and Figure S2 of the supplementary material). Raman modes are tabulated in Table II for CCTO and CCTTO2. In general, the Raman mode frequencies in inorganic transition metal oxides are affected by the asymmetry, effective charge and bond lengths of participating atoms and atomic motions. In this study, we observed five Raman modes for CCTO, *viz* at 290 (F_g), 445 (A_g), 453 (E_g), 511(A_g) and 575 (F_g) for $Im\bar{3}$ crystal symmetry as reported by Kolev *et al* (Figure. 3a).[20] We had carried out Raman mode analysis for *I*4/*mmm* (4/*mmm*) site symmetry as $CaCu_3Ti_{4-x}Te_xO_{12}$ yielded a total of 20 Γ–point modes as shown in Table III. Out of these, 12 modes ($3A_{1g}+ 3B_{1g}+ 2B_{2g}+ 4E_g$) are expected to be Raman active. In Table II, CCTTO2 Raman modes have been assigned based on the earlier reports on Raman studies for tetragonal *I*4/*mmm* crystal structure of AFe_2As_2 and Sr_2RuO_4 ($Sr_3Ru_2O_7$).[21,22]

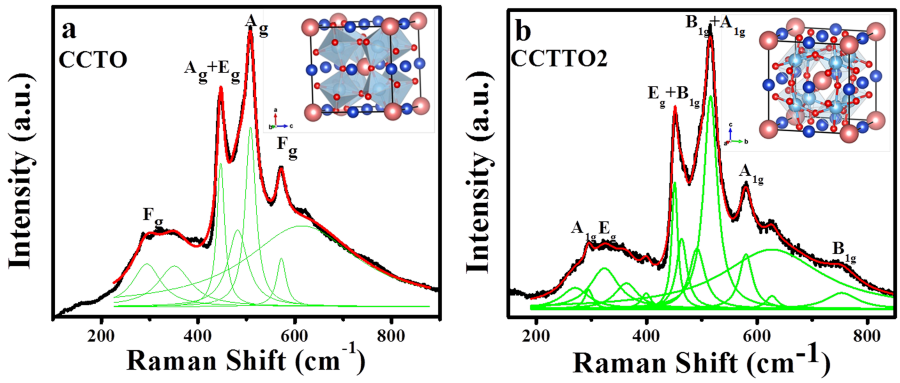

FIG. 3. Room Temperature Raman spectra for $CaCu_3Ti_{4-x}Te_xO_{12}$ where, (a) $x = 0$ and (b) $x = 0.2$. Insets are unit cell model of $CaCu_3Ti_4O_{12}$ and $CaCu_3Ti_{3.8}Te_{0.2}O_{12}$.

TABLE II. List of experimental mode frequencies for $CaCu_3Ti_{4-x}Te_xO_{12}$ (x = 0, 0.2).

$CaCu_3Ti_4O_{12}$		$CaCu_3Ti_{4-x}Te_xO_{12}$ (x = 0.2)	
Exp (cm^{-1})	Modes	Exp (cm^{-1})	Modes
292	F_g	274	A_{1g}
445	A_g	294	E_g
453	E_g	443	E_g
511	A_g	455	B_{1g}
575	F_g	482	B_{1g}
		508	A_{1g}
		572	A_{1g}
		752	B_{1g}

We observed eight prominent modes, which are at 274, 295, 443, 455, 482, 508, 572 and 752 cm^{-1} for CCTTO2. The peaks at 295 (E_g), 443 (E_g), 455 (B_{1g}), 482 (B_{1g}), 508 (A_{1g}) and 572 (A_{1g}) cm^{-1} are due to rotational and stretching/bending modes of TiO_6. For doped samples, the expected TeO_6 octahedral rotation was found in the spectra with the signature peaks assigned to 274 (A_{1g}) and 752 (B_{1g}) cm^{-1}. Multiple peak fitting analysis of Raman spectra for CCTTO2 sample (Figure. 3b) reveals some additional broad Raman peaks around 254, 360, 390, 619 and 662 cm^{-1} with widths greater than 30 cm^{-1}, indicating the mixing of rotational and stretching modes for both the TeO_6 and TiO_6 octahedra. The Raman peaks at 455 cm^{-1} and 482 cm^{-1} in CCTTO2 samples could be attributed to the B_{1g} modes of TiO_6 units. In pure CCTO single crystals, both these peaks are observed at lower temperatures and tentatively assigned to the distorted TiO_6 octahedra (or TiO_5 units) forming twin boundaries in the system.[20] In the present case, partially replacing Ti by Te induces more distortion in BO_6 octahedra which facilitates the formation of twin boundary layers, reflected in room temperature Raman spectra of CCTTO2 samples (Figure. 3b). These peaks are assigned to anti-stretching modes of Ti–O bond of TiO_5 units;[23] which are unambiguously related to off-centre displacement of Ti in the octahedral structure (distortion in BO_6 unit of perovskite lattice).[20]

In order to explain the incipient ferroelectric phenomena in Te doped CCTO samples at low temperatures, Raman studies on CCTTO2 (Figure 4) and CCTTO1 (Figure S3 of the supplementary material) ceramics were conducted at a low temperature. Figure 4 shows the temperature dependent Raman spectra of CCTTO2. Figure 4a shows the Raman peaks above 400 cm^{-1} and Figure 4b shows the Raman peaks below 350 cm^{-1}. In Figure 4a, the peaks in the high frequency region (400–580 cm^{-1}) are ascribed to the internal modes of the TiO_6 octahedra. Figure 4b shows the external modes (100–350 cm^{-1}). This region is related to the Ti^{4+}, Te^{4+} ions and their cooperative motion with oxygen over the whole lattice. We noticed that below 170 K new modes are appearing around 117cm^{-1}, 153cm^{-1}, 246 cm^{-1} and 252 cm^{-1}; *i.e.* related to translational and rotational modes of TeO_6 (lattice modes).[24] Figure 5 shows the temperature dependence of external modes of Ti–O

TABLE III. Wyckoff positions and irreducible representations for $CaCu_3Ti_{4-x}Te_xO_{12}$, space group (*I*4/*mmm*, No.139) which yield Brillouin zone center modes.

Atom	Wyckoff positions			Γ-point phonon modes
Ca1(2a)	0	0	0	$E_u+ A_{2u}$
Cu1(2b)	0	0	0.5	$E_u+ A_{2u}$
Cu2(4c)	0	0.5	0	$2E_u+A_{2u}+ B_{2u}$
Ti(8f)	0.25	0.25	0.25	$3E_u+A_{1u}+2A_{2u}+ 2B_{1u} +B_{2u}$
Te(8f)	0.25	0.25	0.25	$3E_u+A_{1u}+2A_{2u}+ 2B_{1u} +B_{2u}$
O1(8h)	0.2892	0.2892	0	$E_g+2E_u+A_{1g}+A_{2g}+A_{2u}+ B_{1g} +B_{1u} +B_{2g}$
O2(16n)	0	0.1867	0.3218	$3E_g+3E_u+2A_{1g}+A_{2g}+A_{1u}+2A_{2u}+ 2B_{1g} +B_{1u} + 2B_{2u}+B_{2g}$
Raman Active Modes: ($3A_{1g}+ 3 B_{1g}+2 B_{2g}+4E_g$)				
IR Active modes: ($12E_u+ 7A_{2u}$)				

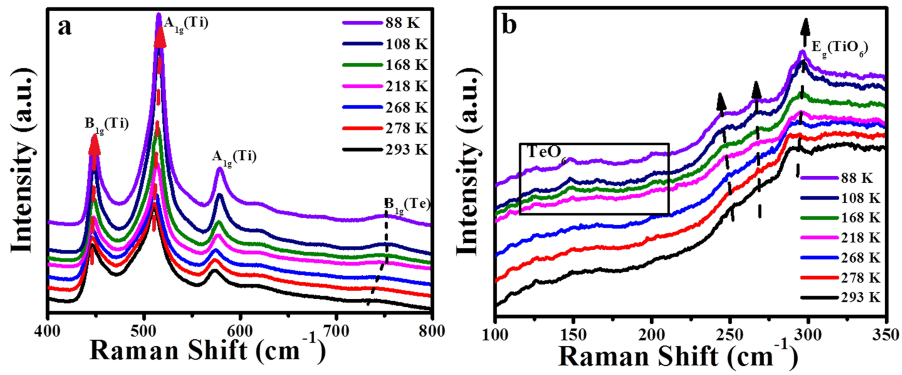

FIG. 4. Temperature dependent Raman measurements for $CaCu_3Ti_{4-x}Te_xO_{12}$ (x = 0.2) (a) high frequency region (400 - 800 cm^{-1}) (b) low frequency region (100 - 350 cm^{-1}).

and Te–O octahedra for CCTTO2 samples (see Figure S3 for corresponding data of CCTTO1). In the case of both the stretching modes (A_{1g} modes at 509 and 572 cm^{-1}), we observe a very little dispersion on changing the temperature up to 270 K, below which there is an unusual hardening of the modes up to 170 K followed by yet another dispersion-less (saturation) behaviour in the temperature range of 170–120 K (see Figure 5a and 5b). Below 120 K, these modes begin to harden again. It is interesting to see that the FWHM of the A_{1g} modes (shown in Figure S4 of the supplementary material) shows anomalous behaviour around 120 K. It should be noted that FWHM of Raman modes is associated with the lifetime of the phonons. There is a decrease followed by an increase in lifetime across 120 K. This suggests the incidence of a possible second order phase transition around this temperature.

The Raman behaviour of A_{1g} modes should be compared with the temperature dependent dielectric behaviour of CCTTO2. As seen in Figure 2a, the relative permittivity study carried out

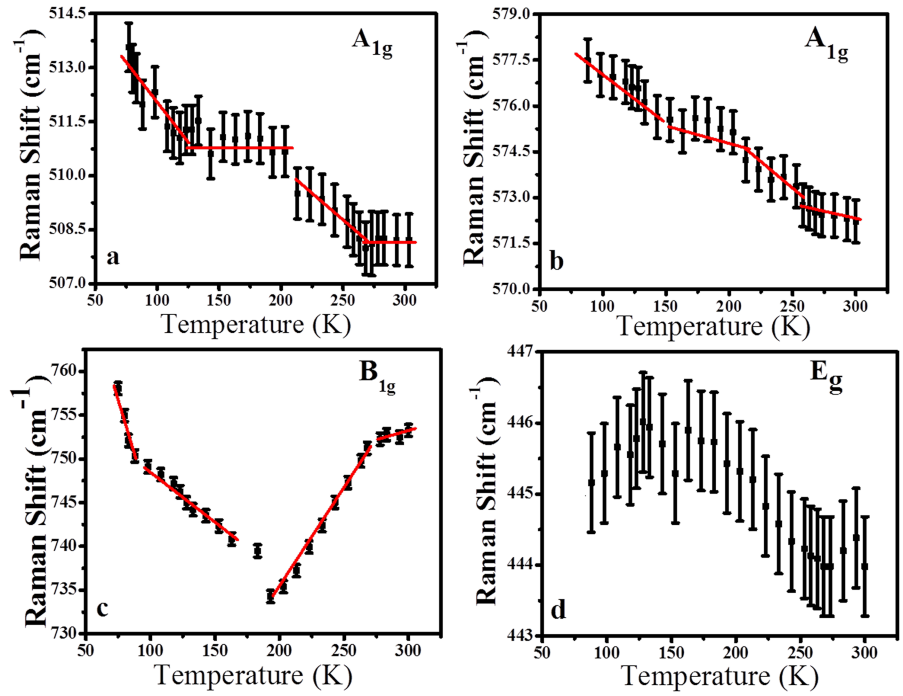

FIG. 5. Raman shift *vs* Temperature for $CaCu_3Ti_{3.8}Te_{0.2}O_{12}$, (a) TiO_6 A_{1g} at 509cm^{-1};(b) TiO_6 A_{1g} at 572cm^{-1}; (c) TeO_6 B_{1g} at 752cm^{-1}; (d) TiO_6 E_g at 443cm^{-1}.

as a function of temperature demonstrates almost temperature independent behaviour up to 270 K, followed by a sharp increase in relative permittivity up to 170 K. Subsequently, there is a sluggish increase in permittivity in the 170–120 K temperature range. Below 120 K, we observe a decrease in permittivity. The above results suggest that the A_{1g} stretching modes have a strong influence on dielectric polarization (polarizability of chemical units) of TiO_6 octahedra. Therefore, it was necessary to look at the temperature dependence of B_{1g} mode of TeO_6 octahedra because of the influence of lone pair of Te^{4+} on the local polarizability. As shown in Figure 5c, B_{1g} mode at 752 cm^{-1} shows temperature independent behaviour up to 270 K, below which it softens anomalously, where the trend of Raman shift is exactly opposite to that of A_{1g} modes of TiO_6 up to 170 K. Below 170 K, it starts to harden with an abrupt jump and again there is a sudden increase in the hardening below 120 K. In the case of E_g mode at 443 cm^{-1} (see Figure 5d), there is an expected anharmonic behaviour up to 120 K and begins to soften below this temperature.

We know that the polarizability associated with chemical units (in double perovskites, mainly BO_6 octahedra) affects the dielectric polarization in a system. Therefore, the anomalous temperature dependent behaviour of stretching and bending modes of TiO_6 and TeO_6 octahedra in CCTTO2 system has a direct influence on the overall polarization vis-à-vis the relative permittivity of the system. On cooling, it is noticed that all the stretching modes of BO_6 octahedra, at first, show temperature invariant behaviour in the temperature range of 300 to 270 K owing to the Ti and Te positions in BO_6 octahedra remaining intact; *i.e.*, the strain associated with TiO_6 and TeO_6 octahedra does not change in this temperature range. The relative permittivity of this system also shows an invariant behaviour in the 300–270 K temperature range. But below 270 K, in the case of dielectric spectra, we notice a sudden increase up to 170 K. In the same temperature range (270–170 K), Raman stretching modes associated with TiO_6 octahedra show normal hardening, but TeO_6 octahedra show softening of the modes. The TeO_6 octahedra relax by strain release (softening/relaxation of Te–O bonds) causing more distortion (Ti–O bond hardening/becomes more rigid) to TiO_6 octahedra. The lone pair associated with Te^{4+} ion along with distorted BO_6 octahedra form micro-clusters of local dipoles (polar ordering) which contribute to the polarization increase in the system resulting in an increase in the dielectric constant upon cooling (incipient ferroelectric behaviour). Below 170 K, further relaxation in Te–O bond is led to stiffening of TeO_6 octahedra which accounted for B_{1g} mode hardening below. The strain relaxation pertaining to TiO_6 octahedra is responsible for the saturation of TiO_6 stretching modes in the 170-120 K temperature range. Due to this competing effects of microclusters of TiO_6 octahedra and nano-polar region induced by Te^{4+}/Ti^{4+}, Cu^{2+}/Ti^{4+}, Cu^{2+}/Te^{4+} couples,[15] the dielectric polarization shows a sluggish increase in this temperature range.

Small amount of impurity (dopants) in incipient ferroelectric systems could induce ferroelectricity.[25,26] For example, above some critical dopant concentrations (x_c), incipient ferroelectric systems like $KTa_{1-x}Nb_xO_3$, $Sr_{1-x}Ca_xTiO_3$ *etc.*, show ferroelectric phase transitions studied using their respective dielectric spectra. A widely accepted viewpoint about the ferroelectric behaviour in incipient ferroelectric-based solid solutions is referred to as an off-center position of impurity ions, producing electric dipoles. But, the experimental data analyses, corroborated with single off-center displacement model of dopants in different incipient ferroelectrics, show a serious limitation as weak off-center positions of heavy dopants lead to low barrier multiwall potentials. Vikhnin *et.al.*[25] had proposed an alternative model to explain the origin of polar ordering in incipient ferroelectric materials and the nature of the ferroelectric transitions due to dopants. According to this model, interaction between the low frequency quasi-local modes in self-organized structurally ordered compositional micro-clusters (reorientation of local dipole moments) and off-centered position of dopants in host lattice of incipient ferroelectric systems are the origin of order-disorder or displacive ferroelectric transitions in these incipient ferroelectric materials.[26,27] Tellurium doped calcium copper titanate forms structurally ordered *I*4/*mmm* double perovskite lattice. The origin of polar ordering upon cooling is attributed to self-organized structurally ordered compositional micro-clusters (resulted from different chemical bonding and steric effect of lone pair) in doped CCTO.

Furthermore, the new lattice modes in the low frequency region (around 117cm^{-1}, 153cm^{-1}, 246 cm^{-1} and 252 cm^{-1}) associated with the relaxation of TeO_6 octahedral are noticed in Raman spectra in the temperature range of below 170 K (see Figure 4b). The intensities of the peaks pertaining to new lattice modes are weak around the transition temperature region (~120 K) indicating that

the interactions between these quasi-local cluster vibrations and the host lattice are short range in nature. The FWHM of the A_{1g} modes (Figure S4 of the supplementary material) shows anomalous behaviour around 120 K. The FWHM of Raman modes reflects on the lifetime of the phonons and shows a decrease followed by an increase in lifetime across 120 K for the doped samples. All the stretching modes of BO_6 octahedra around 120 K show a sudden hardening as confirmed by an anomalous behavior in FWHM (Figure 5 and Figure S4 of the supplementary material). Concurrently, the bending mode of TiO_6 octahedra shows softening below 120 K. Across the phase transitions, it is common to observe hardening of stretching modes followed by softening of bending modes coupled with the FWHM change. As the stretching modes have direct influence on polarization of TiO_6 octahedra, hardening of all these modes (stiffening of Ti–O/Te–O bonds) are responsible for a decrease in polarizability of bonds which is reflected on the dielectric properties as there is a decrease in permittivity value below 120 K. The result obtained from Raman spectroscopic studies suggest the incidence of a possible ferroelectric phase transition around 120 K. However, the predicted value (which is not much higher) using the Barrett formula for CCTTO2 is 135 K (T_0). The above facts suggest the possibility of a second order phase transition taking place around this temperature. Appearance of short range quasi-local micro-cluster vibrations modes and nature of the anomaly of FWHM in the Raman spectra suggest the phase transition to be displacive in nature. However, careful and systematic structural studies could provide further insights into this interesting phenomenon.

IV. CONCLUSIONS

In summary, there was a significant enhancement in the relative permittivity of CCTO samples on increasing Tellurium doping concentration up to the permissible doping limits at room temperature. Analyses of temperature dependent permittivity data for Te^{4+} doped samples with Barrett fit confirm increased possible ferroelectric transition temperature, *i.e.*, both FTT and QFT are positive for the centrosymmetric tetragonal perovskite (CCTTO) samples as compared to cubic perovskite (CCTO). Comparison of temperature dependent permittivity and Raman spectroscopic studies revealed that Te^{4+} doping induces more distortion in the BO_6 octahedra leading to higher displacive ionic polarizability in the lattice. The origin of the incipient ferroelectric property in Te^{4+} doped CCTO samples was found to be originating from intrinsic polar ordering associated with BO_6 corner sharing octahedra of the double perovskite lattice. There could be a possible ferroelectric transition at FTT ($T_0 \sim 135$K) as indicated by Barrett fit analyses of permittivity data for CCTTO ceramics. The systematic investigations from *in-situ* temperature dependent Raman peaks confirm that the microscopic origin of second order phase transition ($T_m \sim 120$ K in CCTTO2 samples) in Te^{4+} doped samples could be displacive type owing to the decoupling of the local electric dipoles and internal redox couples in Te^{4+} and Ti^{4+} sublattices.

SUPPLEMENTARY MATERIAL

The Barret's equation linear fitting (Figure S1 of the supplementary material) to the dielectric constant data of Te^{4+} doped calcium copper titanate ($x = 0.1$, CCTTO1) shows a good fit and the results are shown in the Table I. Raman spectroscopic data (Figure S2) for CCTTO1 samples also shows the peaks corresponding to *I*4/*mmm* tetragonal phase. Figure S3 shows the temperature dependence of external modes of Ti–O and Te–O octahedra for CCTTO1 samples. The FWHM of the A_{1g} modes in Figure S4 shows anomalous behaviour around 120 K which signifies the suspected phase transition.

ACKNOWLEDGMENTS

We thank Ministry of Human Resource and Development, India for the research funding and Indian Institute of Science for the instrument facility. We would also like to acknowledge JNCASR and DST, India for funding.

[1] C. H. Ahn, T. Tybell, and J. M. Triscone, Appl. Phys. Lett. **75**, 856 (1999).
[2] R. Guo, L. You, Y. Zhou, Z. Shiuh Lim, X. Zou, L. Chen, R. Ramesh, and J. Wang, Nat. Comm. **4**, 1990 (2013).
[3] J. F. Scott, Science **315**, 954 (2007).

[4] C. Cancellieri, A. S. Mishchenko, U. Aschauer, A. Filippetti, C. Faber, O. S. Barišić, V. A. Rogalev, T. Schmitt, N. Nagaosa, and V. N. Strocov, Nat. Comm. **7**, 10920 (2016).
[5] S. V. Aert, S. Turner, R. Delville, D. Schryvers, G. V. Tendeloo, and E. K. H. Salje, Adv. Mater. **24**, 523 (2012).
[6] F. A. Miranda, C. H. Mueller, G. A. Koepf, and R. M. Yandrofski, Supercond. Sci. Technol. **8**, 755 (1995).
[7] Yu. A. Boikov, Z. G. Ivanov, A. L. Vasiliev, I. Pronin, E. Olsson, and T. Claesson, Appl. Phys. Lett. **76**, 2708 (1995).
[8] O. G. Vendik and S. P. Zubko, J. Appl. Phys. **82**, 4475 (1997).
[9] O. E. Kvyatkovskioe, Phys. Solid State **43**, 1401 (2001).
[10] V. Trepakovtt, F. Smutny, V. Vikhnin, V. Bursian, L. Sochava, L. Jastrabik, and P. Symikov, J. Phys. Cond. Mat **7**, 3765 (1995).
[11] V. V. Lemanov, A. V. Sotnikov, E. P. Smirnova, and M. Weihnacht, Appl. Phys. Lett. **81**, 886 (2002).
[12] M. C. Ferrarelli, D. C. Sinclair, A. R. West, H. A. Dabkowska, A. Dabkowski, and Gr. M. Luke, J. Mater. Chem. **19**, 5916 (2009).
[13] M. Li, A. Feteira, D. C. Sinclair, and A. R. West, Appl. Phys. Lett. **91**, 132911 (2007).
[14] M. C. Ferrarelli, D. Nuzhnyy, D. C. Sinclair, and S. Kamba, Phys. Rev. B. **81**, 224112 (2010).
[15] N. Barman, S. Tripathi, N. Ravishankar, and K. B. R. Varma, Solid State Comm. **241**, 7 (2016).
[16] G. V. P. Kumar and C. Narayana, Current Science **93**, 778 (2007).
[17] R. Schmidt and D. C. Sinclair, Chem. Mater. **22**, 6 (2010).
[18] J. H. Barrett, Phys. Rev. **86**, 118 (1952).
[19] S. Krohns, P. Lunkenheimer, S. G. Ebbinghaus, and A. Loidl, Appl. Phys. Lett. **91**, 022910 (2007).
[20] M. C. Ferrarelli, D. Nuzhnyy, D. C. Sinclair, and S. Kamba, Phys. Rev. B. **81**, 224112 (2010).
[21] A. P. Litvinchuk, V. G. Hadjiev, M. N. Iliev, B. Lv, A. M. Guloy, and C. W. Chu, Phys. Rev. B **78**, 060503 (2008).
[22] M. N. Iliev, V. N. Popov, A. P. Litvinchuk, M. V. Abrashev, J. Backstrom, Y. Y. Sun, R. L. Meng, and C. W. Chu, Physica B **358**, 138 (2004).
[23] E. A. V. Ferri, J. C. Sczancoski, L. S. Cavalcante, E. C. Paris, J. W. M. Espinosa, A. T. de Figueiredo, P. S. Pizani, V. R. Mastelaro, J. A. Varela, and E. Longo, Mater. Chem. Phys. **117**, 192 (2009).
[24] A. Koitzsch, G. Blumberg, A. Gozar, B. Dennis, A. P. Ramirez, S. Trebst, and S. Wakimoto, Phys. Rev. B. **65**, 052406 (2002).
[25] V. S. Vikhnin, P. A. Markovin, and W. Kleemann, Ferroelectrics **218**, 85 (1998).
[26] P. Barone, D. Di Sante, and S. Picozzi, Phys. Rev. B. **89**, 144104 (2014).
[27] Y. Gu, N. Wang, F. Xue, and L. Q. Chen, Phys. Rev. B. **91**, 174103 (2015).